Voltage quality performance improvement of a distribution feeder with Superconducting Fault Current Limiter

Ming-Tang Chen and Chi-Hung Nguyen

Department of Electrical Engineering, National Kaohsiung University of Applied Sciences
Kaohsiung 807-78, Taiwan, R.O.C
mtchen@cc.kuas.edu.tw and ngchihung78@gmail.com

Abstract: Due to the rapid growth of load demand, different power sources are added to the power system, and the interconnection among various power devices for a modern electric grid also becomes more and more complicated. Therefore, the fault current is dramatically increasing, and Superconducting Fault Current Limiter (SFCL) has introduced to solve the related problems. In this paper proposes the strategies of applying SFCL to distribution feeder for the system performance improvement of power quality, including the fault current limiter and the mitigations of voltage variations including sag and swell. And the effectiveness for different feeder types, radial and closed-loop structures, is analyzed for Taiwan Power Company (Taipower) system. When a single-phase to ground fault happens to a certain point along the feeder or at the tie breaker, the simulation results show that SFCL can effectively limit the fault current, and the decrease in amplitude can be up to approximately 55%. Besides, the research results illustrate that the voltage sag severity at fault phase and voltage swell at non-fault phase are dependent of fault location. Therefore, the effectiveness of voltage quality improvement is definitely illustrated by the curve of Information of Technology Industry Council (ITI Curve).

Keywords: SFCL, power quality, voltage variation, distribution feeder.

1. Introduction

With the increase of electricity consumption nowadays, the electric power system is getting more and more complicated. As a result, the size of the single-line to ground fault that arise from complication of electric power system is increasing. The fault current levels may soon cross the rated fault current breaking capacity of the existing circuit breakers. Therefore, improving the reliability and security of power distribution in the power grids is an important and difficult task. SFCL offer an excellent solution for the increased level of short circuits in power systems, which can improve the stability of the power system. And various types of SFCLs are implemented at substation of power distribution system in real world power grids of many countries [1-6].

SFCL is innovative electric equipment based on the principle of superconductivity. SFCL is an attractive device that limits the short-circuit current rapidly and effectively without affecting the power system during a normal time. In addition, SFCL can enhance voltage quality not only in fault phase but also in non-fault phase when a single-phase to ground fault happened.

Today, power quality problem is one of the importance issues in power system. One of the most significant issues regarding power quality is voltage sag, swell [7]. Voltage sag and swell are incidents in which the voltage amplitude drops and overvoltage for a short time. Generally, the voltage sag and swell can be expressed by the tolerance curve. A popular equipment tolerance curve, the Information Technology Industry Council (ITIC) curve is shown in Figure 1. The first curve, ITIC curve, was formerly called the Computer and Business Equipment Manufacturer Association (CBEMA) [8].

The voltage sag and swell are indicatives of power quality degradation and is a useful measure of the fault events. Nevertheless, there is little progress in the studies on the impact of SFCL's application in improving voltage sag on fault phase and decreasing voltage swell on

Received: January 3rd, 2015. Accepted: March 25th, 2015
DOI: 10.15676/ijeei.2015.7.1.8

non-fault phase during fault in distribution feeder. In this paper, we have evaluated the effects of SFCL on voltage sag and swell of a distribution feeder through study cases which utilizes the ITIC acceptable voltage curve to evaluate the resultant under voltage and overvoltage. It is found that resistive SFCL incorporated in the electric system results in the improvement of voltage drops and reduction of overvoltage, suppressing fault current when a fault occur.

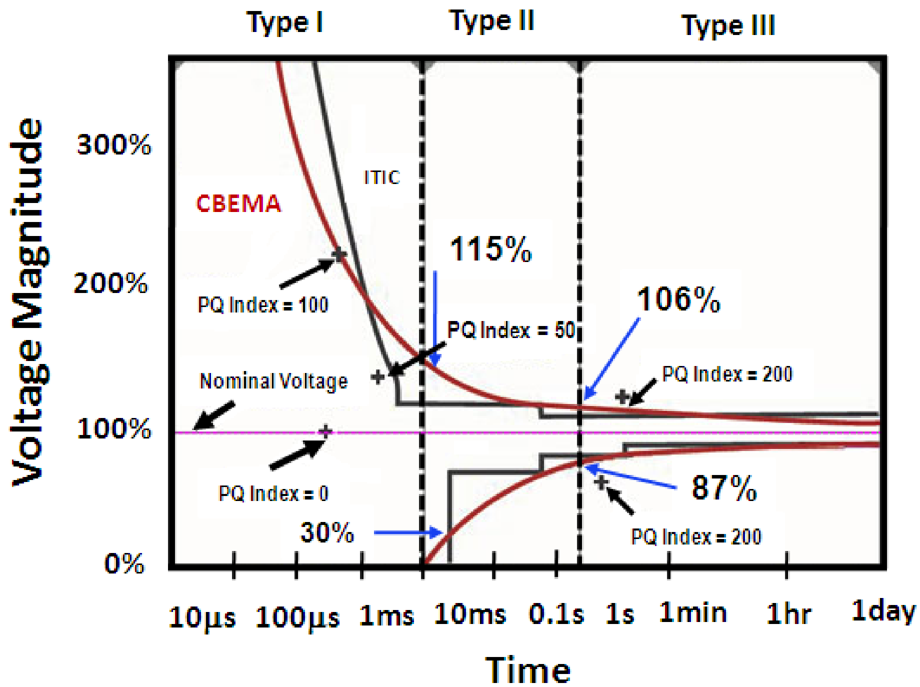

CBEMA (red) and ITIC (black) curves.

Figure 1. Example of tolerance curves with power quality index points.

2. Modeling of resistive SFCL

Many models for SFCL have been developed such as resistive type, reactive type, transformer type, and hybrid type SFCLs [9]. In this study, we defined a resistive type SFCL of Nexans Companies and developed a corresponding MATLAB/Simulink based computer simulation [10-11], and using mathematical expressive equations.

An impedance of SFCL with respect to time t is given by Eqs. (1)-(4).

$$R_{SC}(t) = 0 \qquad (t < t_0), \tag{1}$$

$$R_{SC}(t) = R_m\left[1 - \exp\left(-\frac{(t - t_{0(quench)})}{T_f(I_{fault})}\right)\right]^{\frac{1}{2}} \qquad (t_0 \le t < t_1), \tag{2}$$

$$R_{SC}(t) = \alpha_1(t - t_1) + \beta_1 \qquad (t_1 \le t < t_2), \tag{3}$$

$$R_{SC}(t) = \alpha_2(t - t_2) + \beta_2 \qquad (t \ge t_2) \tag{4}$$

where R_m=1~20 (Ω), T_f=0.01 and t_0 represents the convergence resistance, time constant and quench starting time, respectively. α_1=-80 (Ω/s), β_1=R_m (Ω) and t_1 represents the initial recovery slope, the recovery starting resistance, and recovery starting time, respectively. α_2=-160 (Ω/s), β_2=$R_m/2$ (Ω) and t_2 represents the recovery slope, the second stage recovery starting resistance and recovery starting time, respectively. Quenching is the transition from the superconducting state to the current limiting state of SFCL start at t_0=1sec. Four fundamental parameters are used for modeling resistive type SFCL. The parameters and their values are: 1) transition or response time = 2msec, 2) minimum impedance = 0.01 Ohms and maximum impedance = 20 Ohms, 3) triggering current = 550 A and 4) recovery time = 10 msec [12-13]. If passing current is larger than the triggering current level, the SFCL resistance increases its maximum value. When the current level falls below the triggering current level the system waits until the recovery time and then goes into normal state. Triggering current is the current flowing through the SFCL before fault happened. Figure 2 illustrates resistive SFCL model and the operating characteristics of R_SFCL using MATLAB/Simulink.

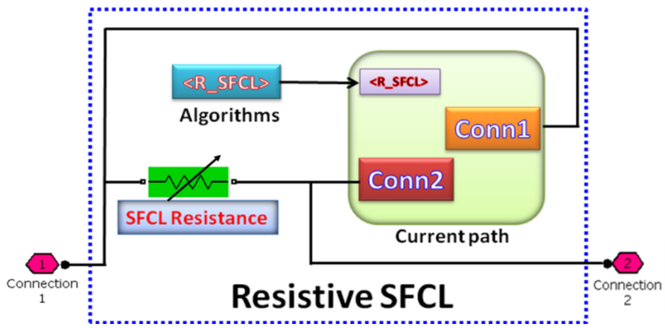

(a) Algorithms and resistive SFCL model designed in simulink.

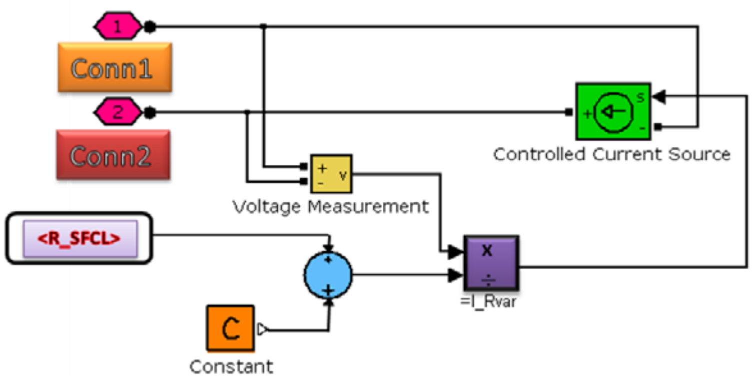

(b) Resistive SFCL characteristics in simulink.

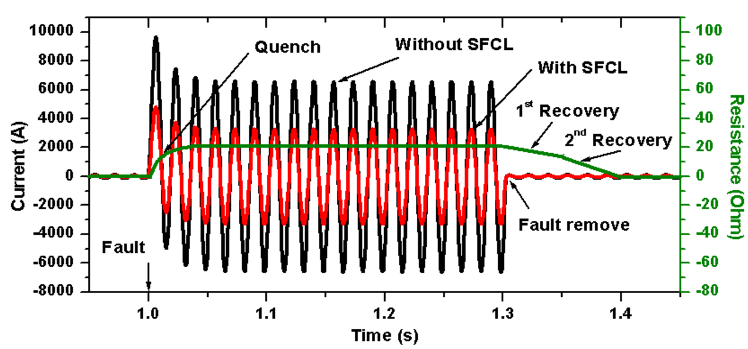

(c) Current and resistance.

Figure 2. Single phase resistive SFCL and simulation results modeled using Matlab/Simulink.

3. Configuration of distribution feeder

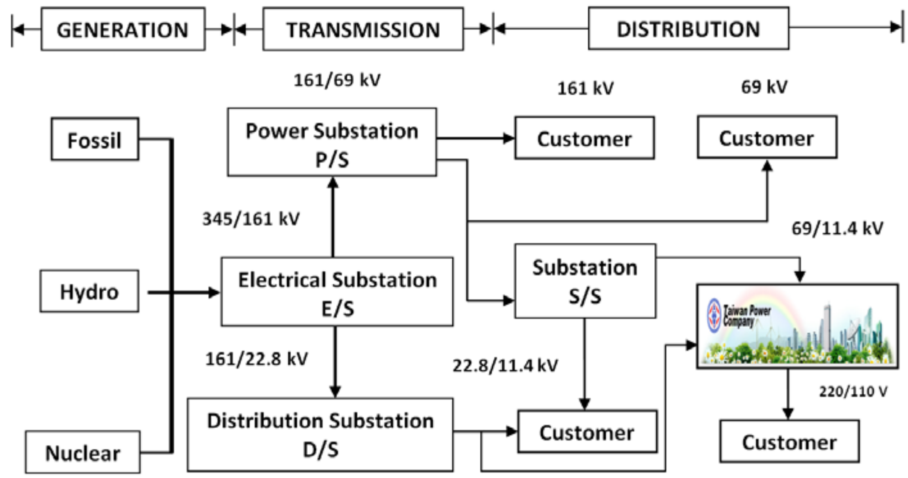

(a) Taipower's system structure.

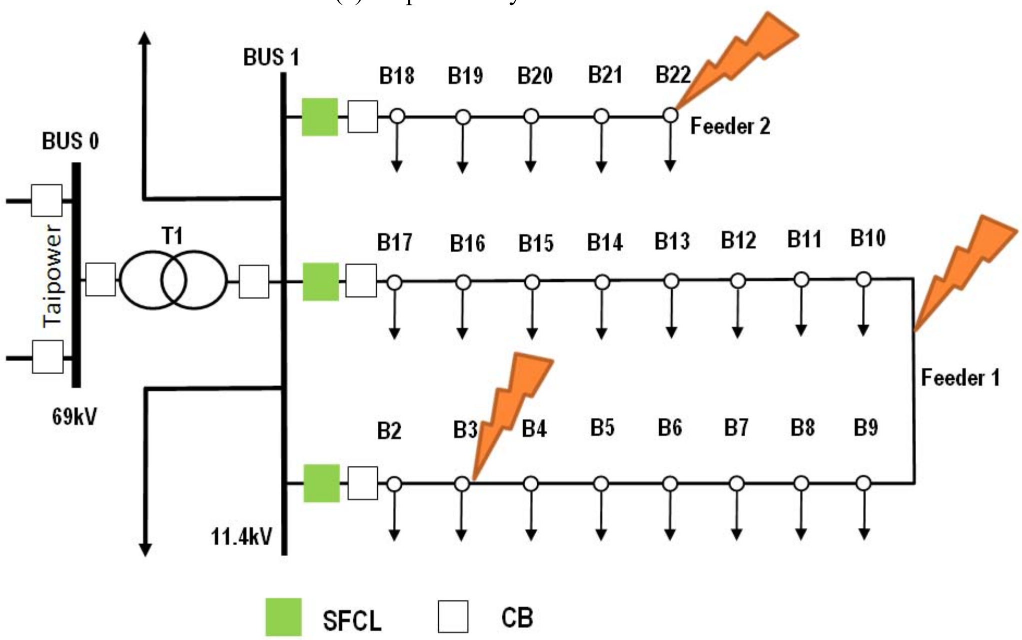

(b) Single-line diagram of the distribution feeder with SFCL.
Figure 3. Structure of Taipower's system and the distribution feeder is selected for study.

One of the distribution substations with a radial feeder and a closed-loop feeder of the Taipower system is selected for study. This set-up consists of main transformer, line, and protective device such as circuit breaker (CB) to protect the system in fault condition, SFCLs to decrease the fault current as shown in Figure 3. Loads group, daily load curves and photograph of the application of SFCL in a distribution feeder as shown in Figure 4. The short circuit capacity at 69kV side of substation is 2976MVA. The distribution transformer (T1) with a rating capacity of 40MVA and an impedance of 9.67% is installed to step-down the voltage level from 69kV to 11.4kV. There are 16 branches point (B2-B17) for the closed-loop feeder and 5 branches point (B18-B22) for the radial feeder. Table 1 gives the line data of the two feeders [14].

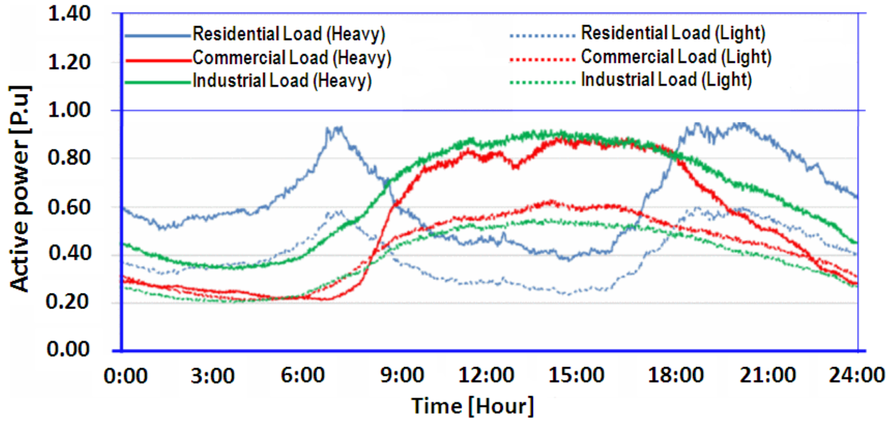

(a) Example of loads.

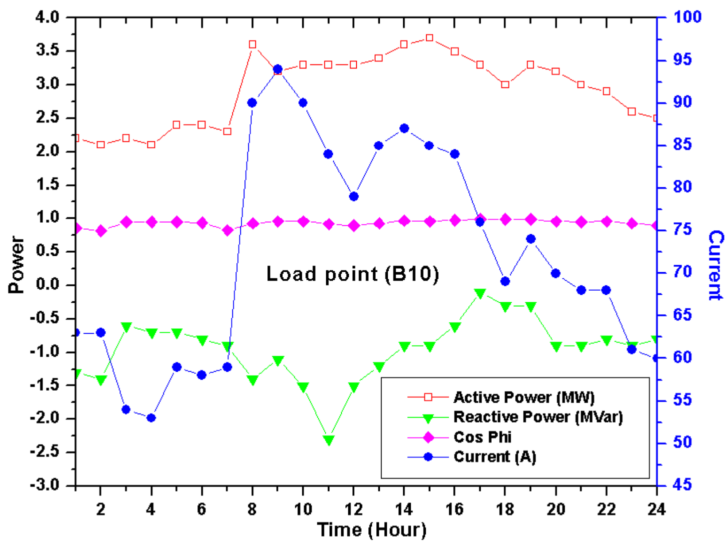

(b) Daily load curves.

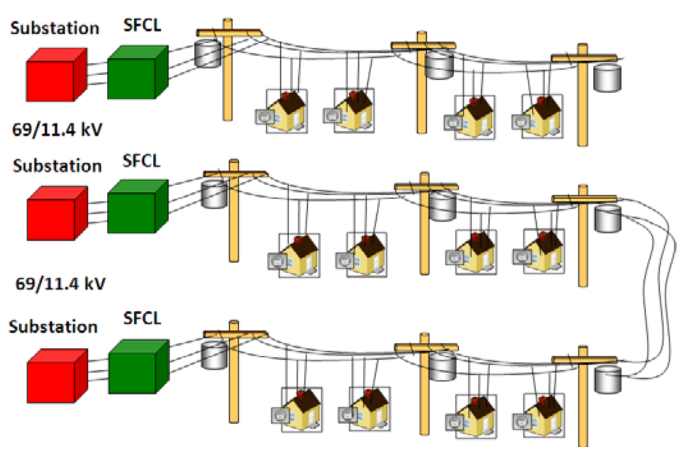

(c) A simplified diagram showing the application of SFCL in a distribution feeder.

Figure 4. Example of load profiles, daily load curves and application of SFCL of a distribution feeder.

Table 1. Distribution line data of the feeders.

From Branch Point	To Branch Point	Conductor Type	Length (km)
2	3	3C500XP2	0.80
3	4	3A477XPW	0.90
4	5	3A477XPW	1.10
5	6	3A477XPW	1.50
6	7	3A477XPW	1.50
7	8	3A477XPW	1.00
8	9	3C500XP2	1.00
9	10	0	0
10	11	3C500XP2	1.00
11	12	3A477XPW	1.00
12	13	3A477XPW	1.50
13	14	3A477XPW	1.50
14	15	3A477XPW	1.10
15	16	3A477XPW	0.90
16	17	3C500XP2	0.80
18	19	3C500XP2	2.25
19	20	3A477XPW	2.25
20	21	3A477XPW	2.25
21	22	3A477XPW	2.25

4. Transient power quality disturbance in power system

Short circuit fault often occurs in power system. It includes three phase short circuit, three phase-to-ground fault, double line-to-ground fault, line-to-line fault, and single line-to-ground fault. Most fault of transmission and distribution systems are single-line to ground fault, making up for about 70-80% of the total number of fault occurrences (According to the data of fault performance recorded by PTC [Power Transmission Companies]), which is the main reason of voltage sag and swell. Single line-to-ground fault can make the power system voltage fluctuate, causing voltage sag, swell, interruption and current swell.

For a single-line to ground fault on phase A, the voltages on phase B and C are Eqs. (5)-(7) [15]:

$$\mathrm{V}_{A\_N} = 0 \tag{5}$$

$$\mathrm{V}_{B\_N} = \mathrm{V}_B - \mathrm{V}_A = \sqrt{3}\mathrm{V}_A \mathrm{e}^{-\mathrm{j}150^0} \tag{6}$$

$$\mathrm{V}_{C\_N} = \mathrm{V}_C - \mathrm{V}_A = \sqrt{3}\mathrm{V}_A \mathrm{e}^{\mathrm{j}150^0} \tag{7}$$

where: V_A, V_B, V_C are the voltage of phase A, B and C, respectively.

Figure 5, Figure 6 and Figure 7 represents the voltage waveform, current at fault point and voltage of power side, respectively on fault phase and non-fault phase without SFCL to illustrate for transient power quality disturbance in power system when a single phase-to-ground happened on phase A at B19 of feeder 2. As seen in Figure 5 the voltage of phase A becomes 0 (short interruption) at the fault point, while voltage of phase B and C voltage swell. In Figure 6 the current of phase A rise high, while phase B and C current swell. Figure 7 shows the voltages of phase A, B, C neighbor fault. As seen in Figure 7, phase A voltage at the power side drops, voltage of phase B and C overvoltage.

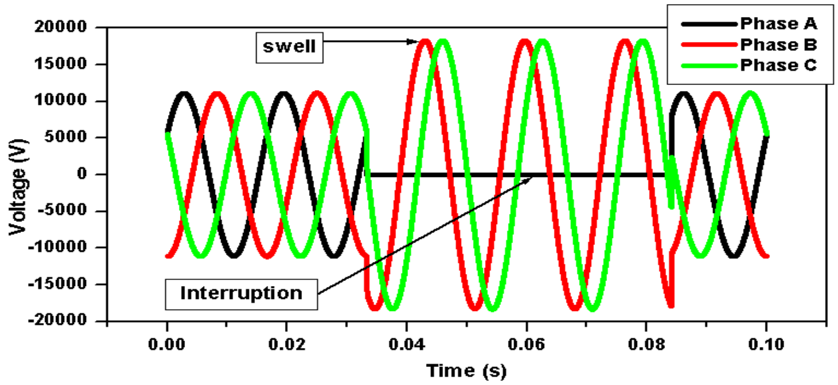

Figure 5. Voltage waveform at fault point for fault at B19 without SFCL.

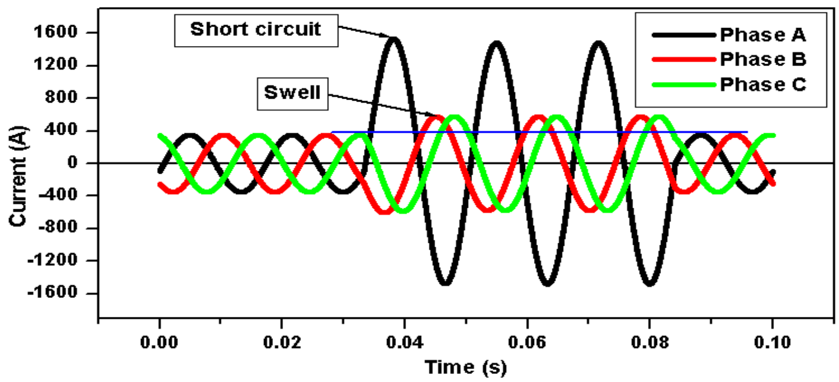

Figure 6. Current waveform at fault point for fault at B19 without SFCL.

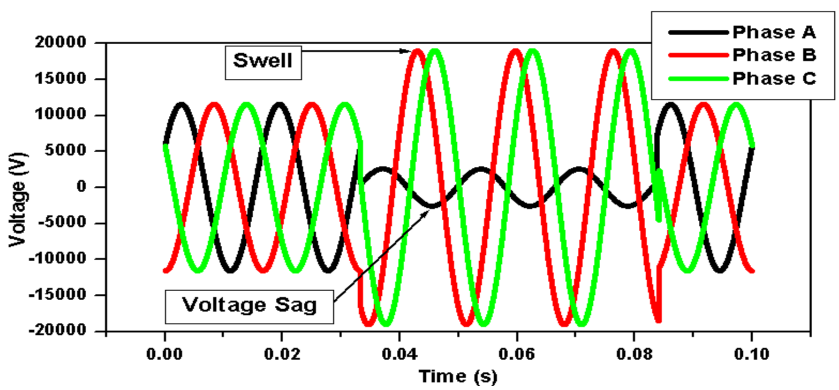

Figure 7. Voltage waveform of power side at B19 without SFCL.

5. Effect of SFCL on voltage quality in distribution system

Generally speaking, a voltage magnitude at bus of output terminal of main transformer during fault can be represented as Eq. (8) if fault impedance is ignored [16].

$$V_{bus} = \frac{Z_L}{Z_{source}+Z_{Tr}+Z_L} \bullet V_{source} \quad (8)$$

where Z_{source}, Z_{Tr}, and Z_L are source impedance, transformer impedance, and line impedance from source to fault location, respectively. While V_{source} is source voltage. Eq. (8) also can approximately represent the voltage magnitude at all neighbor feeders. Different from Eq. (8), Eq. (9) and Eq. (10) are the voltage magnitude when SFCL is installed at two different locations: 1) At output terminal of main transformer or 2) starting point of each feeder.

$$V_{bus} = \frac{Z_L}{Z_{source}+Z_{Tr}+Z_{SFCL}+Z_L} \bullet V_{source} \quad (9)$$

$$V_{bus} = \frac{Z_L+Z_{SFCL}}{Z_{source}+Z_{Tr}+Z_{SFCL}+Z_L} \bullet V_{source} \quad (10)$$

where, Z_{SFCL} means the impedance being statured at normal temperature.

6. Study cases

To evaluate the effect of the SFCL on the voltage sag and swell in a distribution feeder, we used the MATLAB/Simulink software tool to model the components of the described system. Three different scenarios are considered in this paper:

A. Case 1: The faults occurred at any branches point of feeder 2 with SFCL

The main purpose of this study is to discuss the voltage sag and overvoltage from B18 to B22, where the SFCL is installed at starting point and single-phase to ground short circuit can occur at any branches point of feeder 2. Figure 8, Figure 9 presents the voltages waveform at B21, 20, with/without SFCL, respectively. Figure 10 shows current waveform at B22 with/without SFCL, when a fault is created on phase A at t=0.033s at B22 (t=0.00s at starting of the simulation). The CB opened after three cycles and fault clears at 0.083s. Total simulation time was 0.1s. In Figure 10(a) the fault current can be observed to be limited to 771A (56.94%) from 1354A at B22. As seen in Figure 8(a), Figure 9(a) the voltage sag improvement is better in this set up than in the case without SFCL. In addition, voltage sags can be seen increasing from 20.01% (2281V) to 29.95% (3415V), from 39.03% (4450V) to 68.09% (7763V) at B21, 20, respectively. At Figure 10(b), the current swell on non-fault phase limited to 134.49% from 153.98% during fault. As seen in Figure 8(b), Figure 9(b), the voltage swell on non-fault phase has been limited to 132.45% from 158.22% and 122.15% from 152.12% at B21, 20 respectively. Each under voltage and overvoltage events can be characterized by a magnitude and duration and can be plotted as one point in the magnitude duration plane as shown in Figure 11. As seen in Figure 11, without SFCL, the sag events almost dropped below and overvoltage dropped above the suggested voltage tolerance ITIC curve during a fault. By installing SFCL, the voltage sag can be improved at the fault phase, reaching 23% on average, and voltage swell at non-fault phase is lessened. Voltage sag, swell at B18, 19 dropped into the normal operation voltage range of voltage tolerance curve. Figure 12, Figure 13 represents the voltage sag, swell from B18 to B22 when a fault appeared at any branches point of feeder 2. As a result, it is evident from Figure 12 that the voltage sag increases to approximately 26%, 29% at B19, 20 respectively, in Figure 13 the voltage swell decreases to approximately 20% on average.

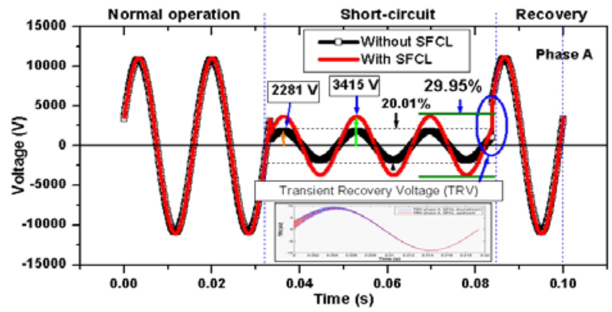

(a) Voltage of phase A at B21.

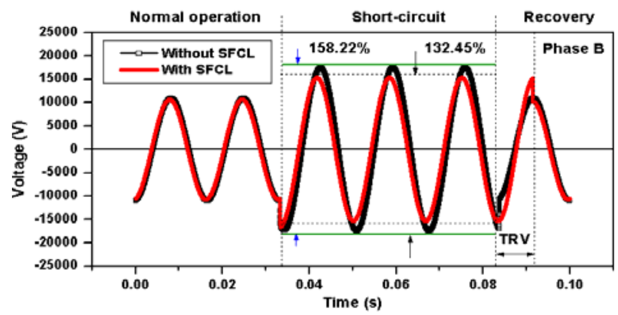

(b) Voltage of phase B at B21.

Figure 8. Voltage waveform at B21with/without SFCL.

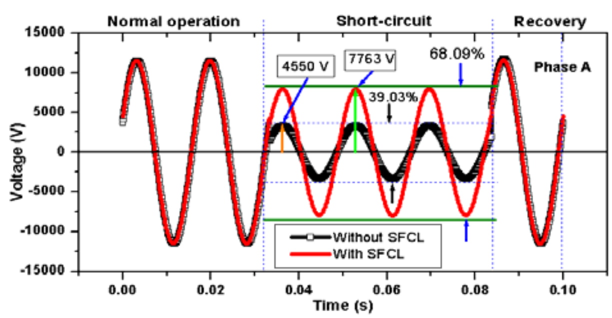

(a) Voltage of phase A at B20.

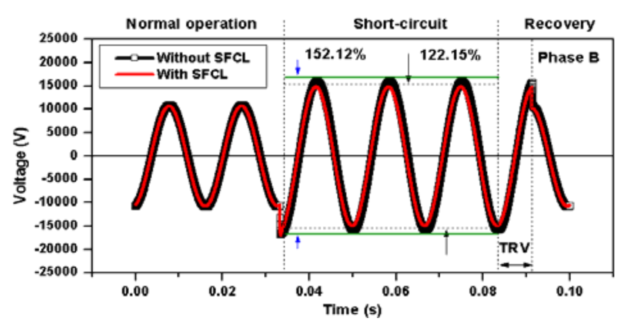

(b) Voltage of phase B at B20.

Figure 9. Voltage waveform at B20 with/without SFCL.

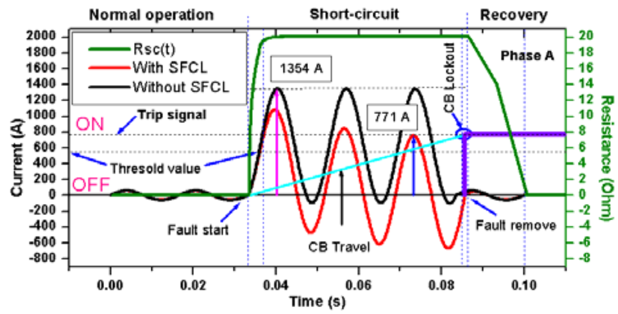

(a) Current of phase A at B22.

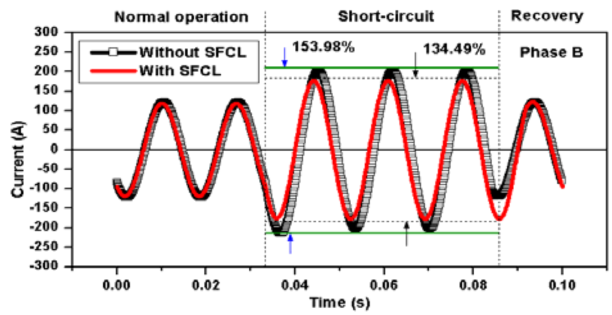

(b) Current of phase B at B22.

Figure 10. Current waveform at B22 with/without SFCL.

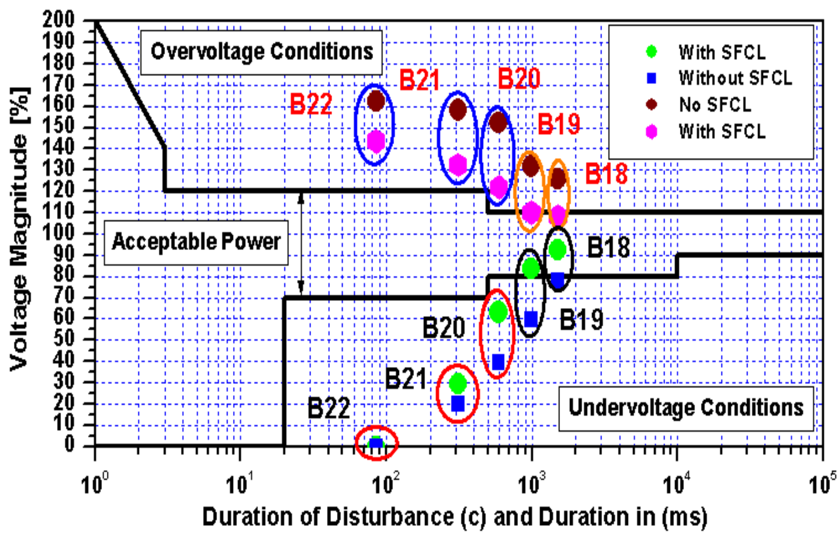

Figure 11. Voltage sag, swell and ITIC curve for study case 1 (the short circuit occurred at B22).

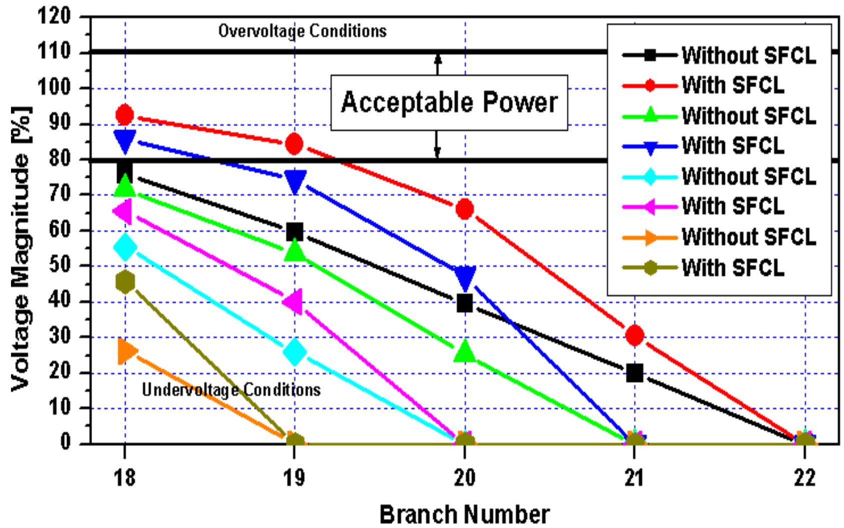

Figure 12. Voltage sags from B18 to B22 with/without SFCL (the faults occurred at any branches point of feeder 2).

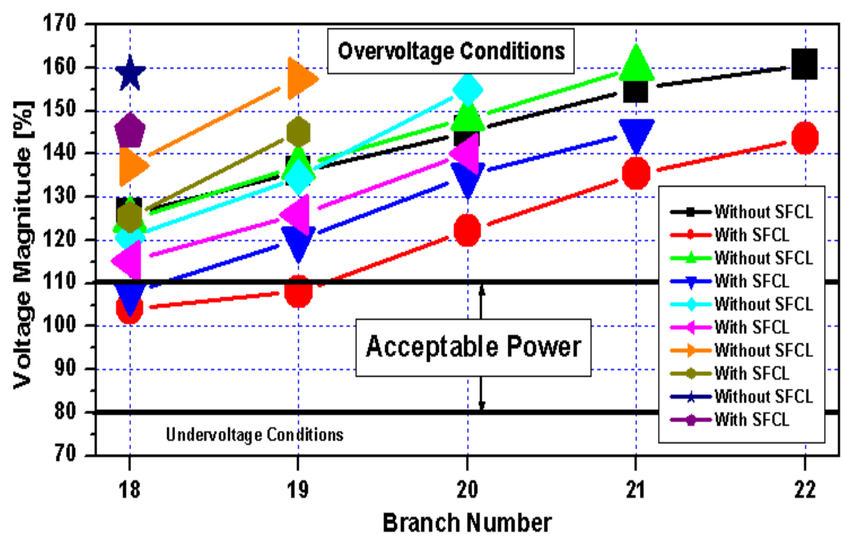

Figure 13. Voltage swells from B18 to B22 with/without SFCL (the faults occurred at any branches point of feeder 2).

B. Case 2: The fault occurred at Tie Breaker of feeder 1 with SFCL

The purpose of the study presented in this section is an analysis of the voltage sag and swell from B2 to B17, where SFCL is installed from starting point to end point of the closed-loop feeder and a fault occurred at tie breaker. Figure 14 illustrates the voltage waveform at B6 with/without SFCL. Figure 15, Figure 16 presents the currents waveform at B9, 10 with/without SFCL, and the accident created at t=0.033s on phase A at tie breaker. The resistive SFCL suppressed fault current and the current flowing through circuit breakers. The CBs opened after 3 cycles and subsequently clears the fault at 0.083s. As seen in Figure 15(a), Figure 16(a) the fault current can be observed to be limited to 915A (53.44%), 805A (54.39%) from 1712A, 1480A at B9, 10, respectively. In Figure 14(a) the voltage sag on fault phase has been improved from 24.82% (2830V) to 50.43% (5750V) at B6 during a fault. At seen in Figure 15(b), Figure 16(b) the currents swell on non-fault phase are limited to 144.32% from

160.02% and 140.32% from 156.06% at B9, 10, respectively. At Figure 14 (b) voltage swell on non fault phase has been limited to 128.93% from 139.95% at B6. Figure 17 gives the sites of the voltage sag, swell events for study case 2. As seen in Figure 17, without SFCL, all the sag events dropped below and voltage swell dropped above the ITIC curve. However, with the insertion of SFCL, the sag events that can be improved and overvoltage are lessened, which dropped into the acceptable power the curve of ITIC are at B2, 3, 4, 15, 16, 17. Figure 18 represents the voltage sag and overvoltage from B2 to B17 when a short circuit occurred at tie breaker. The voltage sag improvement in this case can be increased from 10% to 30%, voltage swell decreased from 10% to 20% along the feeder.

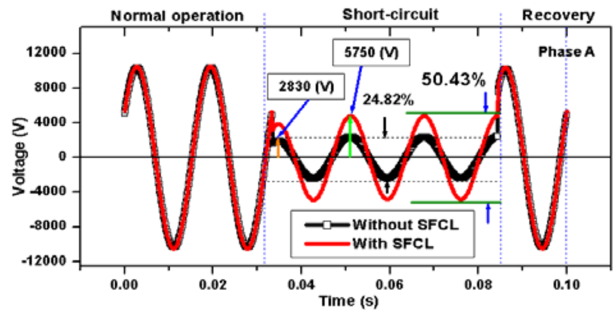

(a) Voltage of phase A at B6.

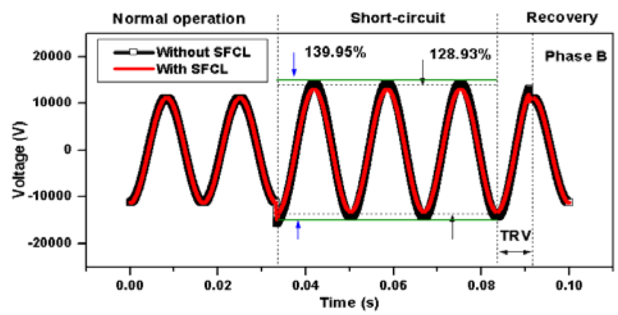

(b) Voltage of phase B at B6.

Figure 14. Voltage waveform at B6 with/without SFCL.

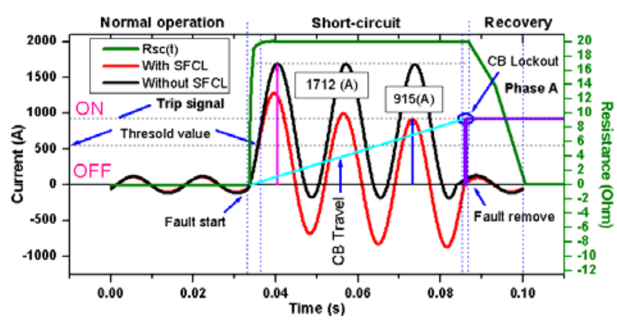

(a) Current of phase A at B9.

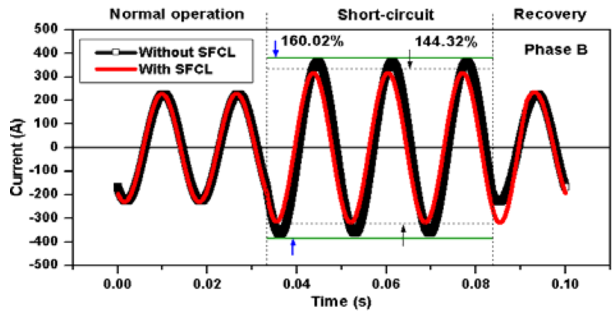

(b) Current of phase B at B9.

Figure 15. Current waveform at B9 with/without SFCL.

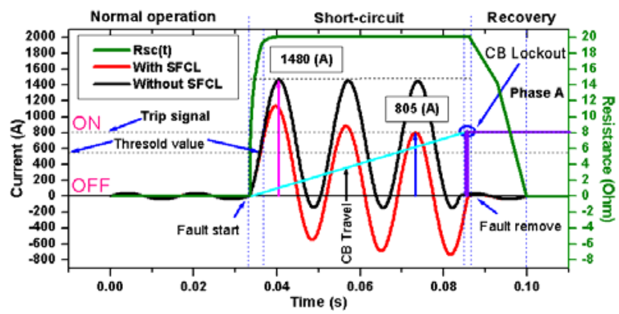

(a) Current of phase A at B10.

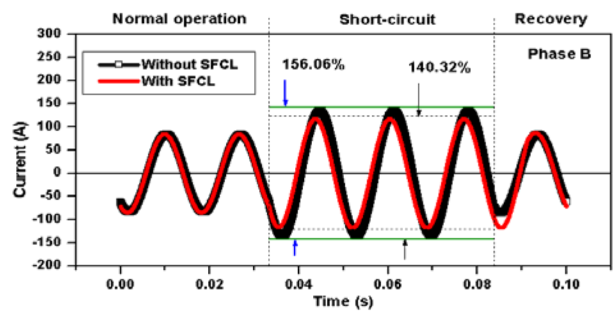

(b) Current of phase B at B10.

Figure 16. Current waveform at B10 with/without SFCL.

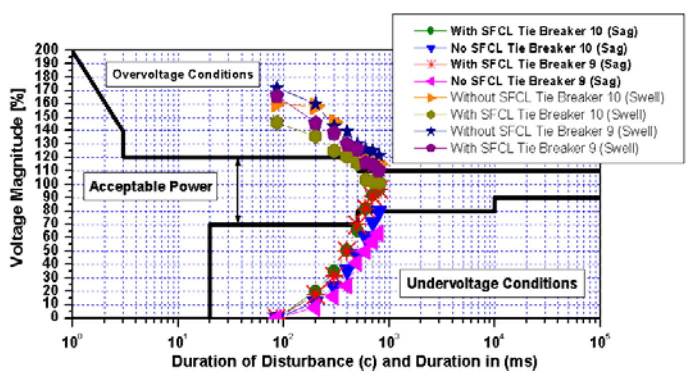

Figure 17. Voltage sag, swell and ITIC curve for study case 2 with/without SFCL (the fault occurred at Tie Breaker of feeder 1).

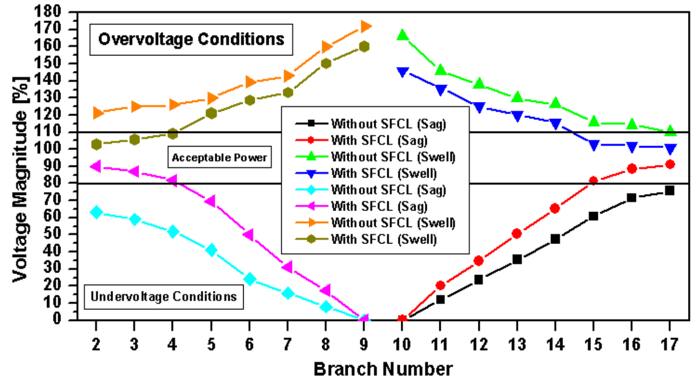

Figure 18. Voltage sag, swell from B2 to B17 with/without SFCL (the short circuit occurred at Tie Breaker of feeder 1).

C. Case 3: The faults occurred at any branches point of feeder 1 with SFCL

This case present the voltage drops and overvoltage analysis from B3 to B17 where SFCL installed from starting point to end point of the closed-loop feeder and the short circuit is created at any branches point of feeder 1. Figure 19 illustrates the voltage sag and voltage swell sites from B3 to B17, when a fault occurred at B3. Using the ITIC curve, Figure 20 represents under voltage and overvoltage, when a short circuit happened at any branches point of feeder 1. As can be observed from Figure 20, without SFCL the voltage sags mostly dropped below and voltage swells dropped above the threshold of voltage tolerance curve. With the installation of SFCL, improvements of voltage sag and swell depended on fault point and length between feeder starting point and fault position. The improvements in voltage sag in this case can be increases to approximately 30%, and voltage swell decreases to approximately 15% at B14.

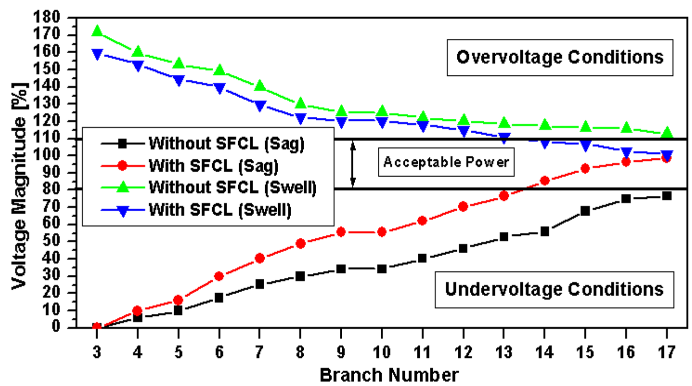

Figure 19. Voltage sag, swell from B3 to B17 with/without SFCL (the short circuit occurred at B3 of feeder 1).

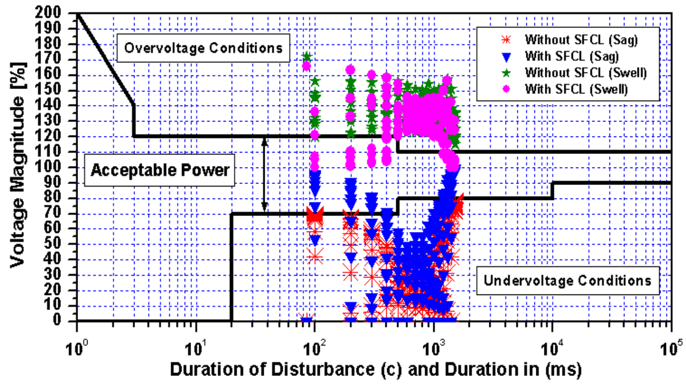

Figure 20. Voltage sag, swell and ITIC curve for study case 3 with/without SFCL (the faults occurred at any branches point of feeder 1).

7. Conclusion

In this paper, we have analyzed and discussed the effect of SFCL on voltage sag and voltage swell in a distribution feeder through some study cases. Under voltage and overvoltage for all cases are evaluated with ITIC curve. Simulation results show that, without SFCL, all the sag events dropped below and voltage swell dropped above the suggested voltage tolerance curve. With the insertion of SFCL, the voltage sag at fault phase can be improved and voltage swell at non-fault phase are lessened, which is depended on fault point and length between feeder starting point and fault location. The effectiveness is such that under voltage and overvoltage at closed-loop feeder is more severe than at radial feeder. As a result, the installation of SFCL improves voltage magnitude of sag and reduces voltage magnitude of swell considerably. In the future studies, various types of faults, protective coordination, and so on should be considered.

8. References

[1] H. R. Kim, S. D. Yu, H. Kim, W. S. Kim, S. E. Yang, J. Y. Lee, and O. B. Hyun, "Demonstration of a Superconducting Fault Current Limiter in a Real Grid," *IEEE Transactions on Applied Superconductivity*, vol. 23, no. 3, p. 5603604, June 2013.

[2] L. Martini, M. Bocchi, M. Ascade, A. Valzasina, V. Rossi, C. Ravetta, and G. Angeli, "Live-Grid Installation and Field Testing of the First Italian Superconducting Fault Current Limiter," *IEEE Transactions on Applied Superconductivity*, vol. 23, no. 3, p. 5602504, June 2013.

[3] C. Zhou, P. Wang and D. Jacobson, "The application of Superconducting Fault Current Limiters in Manitoba Hydro HVDC system," *IEEE Power and Energy Society General Meeting (PES)*, pp. 1–5, 2013.

[4] S. Lee, J. Yoon, B. Yang, Y. Moon and B. Lee, "Analysis model development and specification proposal of 154 kV SFCL for the application to a live grid in South Korea," *Elsevier, Physica C: Superconductivity and its Applications*, vol. 504, pp. 148-152, 2014.

[5] M. Stemmle, F. Merschel, M. Noe and A. Hobl, "AmpaCity Installation of advanced superconducting 10 kV system in city center replaces conventional 110 kV cables," *IEEE 2013 International Conference on Applied Superconductivity and Electromagnetic Devices*, Beijing, China, pp. 323–326, October 2013.

[6] C. S. Song, H. Lee, Y. S. Cho, J. Suh and G. Jang, "Implementation of superconducting fault current limiter for flexible operation in power substation," *Elsevier, Physica C: Superconductivity and its Applications*, vol. 504, pp. 158-162, 2014.

[7] R. C. Dugan, M. F. Granaghan, S. Santoso, H. W. Beaty, "Electrical Power Quality", 2nd Edition, New York, NY, USA: *McGraw Hill*, 2004.

[8] ITI *(CBEMA) Curve Application Note*, Information Technology Industry Council, [Online] Available: http://www.itic.org

[9] L. Wang, P. Jiang and D. Wang, "Summary of Superconducting Fault Current Limiter Technology," *Frontiers in Computer Education, Springer-Verlag Berlin Heidelberg*, AISC 133, pp. 819-825, 2012.

[10] Superconducting Fault Current Limiters http://www.nexans.co.uk/eservice/UK-en_GB/navigate_270512/Superconducting_Fault_Current_Limiters.html

[11] MATLAB Sim Power Systems, Mathworks, 2014. http://www.mathworks.com/products/simpower/

[12] U. A. Khan, W. J. Shin, J. K. Seong, S. H. Oh, S. H. Lee and B. W. Lee, "Feasibility analysis of the application and positioning of DC HTS FCL in a DC micro-grid through modeling and simulation using Simulink and SimPowerSystem," *Elsevier, Physica C: Superconductivity and its Applications*, vol. 47, pp. 1322-1326, 2011.

[13] Feng Zheng, Changhong Deng, Lei Chen, Shichun Li, Yang Liu, and Yuxiang Liao "Transient Performance Improvement of Microgrid by a Resistive Superconducting Fault Current Limiter," *IEEE Transactions on Applied Superconductivity*, vol. 25, no. 3, p. 5602305, 2015.

[14] Distribution Mapping Management System (DMMS), Taiwan Power Company Annual Research Project TPC-546-4840-9901 (2012) Taiwan Power Co., Ltd. Taiwan, R.O.C. http://www.taipower.com.tw/

[15] Wu Zhu, Wei-Ya Ma, Yuan Gui and Hua-Fu Zhang, "Modelling and Simulation of PQ Disturbance Based on Matlab," *International Journal of Smart Grid and Clean Energy*, Vol. 2, No. 1, pp. 18-24, January 2013.

[16] Y. G. Kim, S. E. Nod, J. S. Kim, J. C. Kim, S. H. Lim and H. R. Kim, "Analysis on Voltage Sag According to Impedance and Application of SFCL with Recloser-Recloser Coordination," *The Transactions of the Korea Institute of Electrical Engineers*, Vol. 63, No. 2, pp. 230-236, 2014.

Ming-Tang Chen was born in Taiwan in 1958. He received his B.Sc. M.Sc. and Ph.D. degrees from Department of Electrical Engineering, National Cheng Kung University (NCKU), Tainan, Taiwan in 1981, 1986, and 1990, respectively. He has been with Department of Electrical Engineering, National Kaohsiung University of Applied Science (NKUAS) since 1992, where he is presently a professor. His research interests are power system, electric quality and he is working on the application of Web-based Virtual Instrumentation to the measurements of various power quality disturbances. Prof. Dr. Chen is currently a member of the Institute of Electrical and Electronics Engineers (IEEE) and president of Shu-Zen Junior College of Medicine and Management (SZMC).

Chi-Hung Nguyen was born in Long An Province Vietnam, on March 10, 1978. He received the B.Sc. and the M.Sc. degrees from the Department of Electrical and Electronic Engineering, University of Technology and Education (UTE), Ho Chi Minh City, Vietnam in 2000 and 2006, respectively. He is currently pursuing his Ph.D. degree at the Department of Electrical Engineering, National Kaohsiung University of Applied Sciences (NKUAS), Kaohsiung, Taiwan. His research interests are power system and quality, application of SFCL to power systems, protective coordination.